Higgs Energy Spheres and Higgs Two-Step Mass Generation

Malcolm H. Mac Gregor*
130 Handley Street
Santa Cruz, CA 95060
February 16, 2014
e-mail: mhmacgreg@aol.com

Abstract

Elementary particles can be represented as localized concentrations of energy, which act as Higgs energy spheres *S*. The sphere radius specifies its energy, and hence its coupling to the scalar Higgs field. Massless photon energy spheres are defined by the Planck equation $E = hv$. Massive particle energy spheres are defined by the *fine structure electrostatic energy equation* and the *fine structure inertial mass equation*, which are derived from the fine structure constant $\alpha \sim 1/137$. Higgs particle generation occurs in two steps: (1) an *electrostatic-energy* sphere is created; (2) it adiabatically expands radially by a factor of 137 and transforms into a Compton-sized *inertial-mass* sphere, which represents a Higgs unit energy quantum. Four Higgs energy channels (electron, boson, fermion and gauge boson) accurately reproduce lepton, constituent-quark, hadron, and average-gauge-boson masses.

PACS numbers: 12.10.Kt, 12.60.Fr, 12.90.+b

*Formerly at Lawrence Livermore National Laboratory

1. Higgs energy spheres *S* as coupling constants to the Higgs energy field

An elementary particle is in essence a stable or metastable *localized concentration of energy*, which is related to its *inertial mass* by the Einstein equation $E = mc^2$. The scalar Higgs field of the vacuum state serves as the *energy source* for the generation of elementary particle masses. The particles themselves can be represented as *Higgs energy spheres S*, which couple to the Higgs field. The energy *E* of a Higgs sphere *S* is determined by its *radius r*, so that the size of the sphere specifies the strength of the particle coupling to the Higgs field.

There are two classes of Higgs energy spheres: *photon spheres* ${}^{\gamma}S_r$, which are associated with *massless* photons; and *alpha spheres* ${}^{\alpha}S_r$, which are associated with *massive* particles, and which involve the fine structure constant $\alpha = e^2/\hbar c \cong 1/137$. The occurrence of the factor 137 is the *signature* for Higgs mass generation.

2. Higgs photon energy spheres

The energy of a photon is given by the Planck energy equation

$$E = h\nu = hc/\lambda = \hbar c/r = 197.33 \text{ MeV-fm}/r_{\text{fm}}, \qquad (1)$$

where $r_{\text{fm}} = \lambda_{\text{fm}}/2\pi$ is the sphere radius in fermis (10^{-13} cm). This equation defines the *Higgs photon energy sphere* ${}^{\gamma}S_{r_{\text{fm}}}$, whose radius r_{fm} determines the energy *E*. Photon energy spheres apply for all photon energies. The volume of the sphere is $V = \frac{4}{3}\pi r^3$, so the energy density in the sphere is $D = (\frac{3}{4\pi})(\hbar c/r^4)$, which varies as $1/r^4$. The energy in an electric field $\vec{\mathrm{E}}$ varies as $1/r^2$, so that $D \propto \vec{\mathrm{E}}^2$. The time-averaged expectation value of the $\vec{\mathrm{S}} = \vec{\mathrm{E}} \times \vec{\mathrm{H}}$ Poynting Vector electromagnetic transport density is $\langle \vec{\mathrm{S}} \rangle = \frac{1}{2}\vec{\mathrm{E}}^2$, so that the *D* and $\langle \vec{\mathrm{S}} \rangle$ electromagnetic energy densities have the same geometric dependence on *r*. Hence the Higgs photon sphere ${}^{\gamma}S_{r_{\text{fm}}}$ has electromagnetic properties that are suitable for an energy coupling constant to the Higgs Field.

3. Higgs alpha-energy spheres and alpha-mass spheres

The equation for the dimensionless fine structure constant alpha is [1]

$$\alpha = e^2/\hbar c \cong 1/137.036000. \tag{2}$$

The constant α is one of the most precisely determined quantities in physics, both experimentally and theoretically. It plays a dominant role in atomic physics, quantum electrodynamics, and condensed matter physics. It also serves as a scaling factor in particle physics, as displayed in the well-known radial array

$$r_{\text{Thomson}} \times 137 = r_{\text{Compton}}, \quad r_{\text{Compton}} \times 137 = r_{\text{Bohr}}\ . \tag{3}$$

The *Thomson radius*, also denoted as the *classical electron radius*, is $r_{Th} = e^2/m_e c^2,$ where m_e is the electron mass. The Compton radius is $r_C = \hbar/m_e c$ The Bohr radius is $a_{\text{o}} = \hbar^2/m_e e^2.$ The significance of this radial array is that it establishes a relationship between the constant α and particle radii and masses (the electron mass).

To obtain an *r*-dependent fine structure equation, $\alpha_r(r)$, we re-write Eq. (2) in the form

$$\alpha_r(r) \equiv \frac{(e^2/r)}{(\hbar c/r)} \cong 1/137, \qquad . \tag{4}$$

which applies for all values of *r*. The (e^2/r) numerator is an *electrostatic energy* term E^{ee}, whose value is determined by the *fine-structure electrostatic-energy equation*

$$E^{ee} \equiv e^2/r = \hbar c/137\, r = 197.33\ \text{MeV}/137\, r_{\text{fm}} = 1.4400\ \text{MeV}/r_{\text{fm}}\,. \tag{5}$$

The electrostatic energy is contained within a sphere of radius *r*, so that Eq. (5) defines the *Higgs alph- energy sphere* ${}^{\alpha}S^{ee}_{r_{\text{fm}}},$ which applies for any value of r_{fm}. In particular, if r_{fm} is the Thomson radius $r_{\text{Th}} = 2.818$ fm, the calculated ${}^{\alpha}S^{ee}_{r_{\text{Th}}}$ energy is $E^{ec} = 0.511$ MeV, the electron energy.

To obtain a fine-structure mass equation $\alpha_m(r_C)$, we first set the radius r_{fm} in Eq. (5) equal to the electron Compton radius $r_C = \hbar/m_e c$, so that

$$\alpha_r(r_C) \equiv \frac{(e^2/r_C)}{(\hbar c/r_C)} \cong 1/137. \tag{6}$$

Then we replace the factor r_C in the denominator with the equivalent value $\hbar/m_e c,$ which gives the *r*-dependent, *m*-dependent fine-structure equation

$$\alpha_m(r_C) \equiv \frac{(e^2/r_C)}{(m_e c^2)} \cong 1/137. \quad (7)$$

Finally, we rearrange Eq. (8) so as to form the electron *fine-structure inertial-mass equation*

$$E^{im_e} = e^2/(r_C/137) = e^2/r_{\mathrm{Th}} = m_e c^2. \quad (8)$$

Eq. (8) defines the *Higgs alpha mass sphere* ${}^{\alpha}S^{im_e}_{r_C}$, which acts as the Higgs coupling constant that determines the electron mass m_e.

4. The Higgs two-step adiabatic alpha-sphere mass generation process

The most distinctive feature of Higgs energy-sphere mass generation is its *two-step* adiabatic transformation of *electrostatic energy* into particle *unit mass* quanta, where the significance of the factor 137 in the mass generation process becomes apparent. Higgs two-step mass generation occurs as an *adiabatic* transformation of a Higgs alpha-energy sphere ${}^{\alpha}S^{ee}_{r_{\mathrm{fm}}}$ into a Higgs alpha-mass sphere ${}^{\alpha}S^{im}_{r_C}$ (Eqs. 5 and 8). The electrostatic radius r_{fm} determines the energy that is extracted from the Higgs field, and the Compton radius r_C determines the size of the inertial mass that is created by the adiabatic energy transformation. This two-step generation process occurs in the creation of *four* generic classes of particle masses: the *electron* mass $m_{\mathrm{e}} = 0.511$ MeV; the *boson* unit mass $m_b = 70$ MeV; the *fermion* unit mass $m_f = 105$ MeV; the *gauge boson* unit mass $m_{gb} = 42.86$ GeV. The electron mass m_e assumes the role of the Higgs *ground state* energy, and α-leaps in energy create the *m*b, m_f and m_{gb} unit energy quanta for the higher-mass particles. Multiples of each of these three unit energy quanta are formed, and they accurately reproduce the energies of the pseudoscalar mesons, the leptons, the six inertial-mass fermion quarks, the proton, the lowest-state vector mesons, and the gauge bosons. These masses are created in coupled particle-antiparticle energy channels that together fulfill the particle conservation rules.

5. The electron two-step energy channel

Higgs energy spheres that represent the two-step electron generation process have radii r_{Thomson} and r_{Compton} that are obtained from Eq. (3), and are displayed in Eq. (8). This equation can be rewritten in terms of the alpha-spheres ${}^{\alpha}S^{ee}_{r_{\mathrm{Th}}}$ and ${}^{\alpha}S^{im_e}_{r_C}$ as the α-transformation equation

$$ {}^{\alpha}S^{ee}_{r_{\text{Thomson}}} \Rightarrow {}^{\alpha}S^{im_e}_{r_{\text{Compton}}}. \tag{9} $$

This equation denotes the two-step process in which 0.511 MeV of electrostatic energy is extracted from the Higgs field in the form of an *energy* sphere of radius $r_{\text{Th}} = 2.818$ fm, and is then adiabatically expanded into an m_e *inertial-mass* sphere of radius $r_C = 386$ fm. This is an increase in volume of $137^3 \cong 2.6\times10^6$, with a corresponding decrease in energy density *D*. A parallel equation occurs for the creation of a positron mass $\bar{m}_e$. The $m_e + \bar{m}_e = 1.022$ MeV pair serves as the ground state for a second two-step Higgs excitation process that creates the π mesons.

6. The Compton spectroscopy of the electron inertial-mass sphere ${}^{\alpha}\mathbf{S}^{\mathbf{im_e}}_{\mathbf{r_C}}$

The electron appears in Eqs. (8) and (9) as a Compton-sized energy sphere of inertial mass m_e. The Compton size is confirmed by the spectroscopic features of the electron—mainly its spin angular momentum *J* and magnetic moment μ—which imply that the mass m_e is uniquely in the form of a relativistically spinning sphere (RSS), whose properties have been well-documented [2-3]. An RSS is a spinning solid sphere whose non-spinning rest mass is m_{o}, and whose equator is moving at (or infinitesimally below) the limiting velocity $\text{v} = c$. Its calculated spinning mass and moment-of-inertia are $m_s = \frac{3}{2}m_{\text{o}}$ and $I = \frac{1}{2}m_s r^2$, which apply for any radius r_i and mass m_i of the RSS. If we now set $m_s = m_e$ and $r = r_C = \hbar/m_e c$, then the calculated spin is $J = \frac{1}{2}\hbar$. A massless point charge *e* placed on the equator acts as a current loop, and has a calculated magnetic moment $\mu = e\hbar/2m_e c$. Thus the electron gyromagnetic ratio is correctly reproduced. The quantities *J* and μ transform correctly under Lorentz transformations if, and only if, the RSS is spinning at the full relativistic limit. These results seem to be mandate a Compton-sized RSS. They apply not only to the electron, but also to spin 1/2 inertial-mass quarks, as demonstrated in the calculation of hyperon magnetic moments [4-5].

7. The boson two-step energy channel and the boson unit mass m_b

About 200 elementary particle states that have been observed experimentally [1], of which 157 have well-determined masses and lifetimes [6]. Most of these particles are strongly-interacting *hadrons* that are formed as combinations of quark states. Three are weakly-interacting *leptons*—the electron, muon and tauon. There are 19 quark and particle "ground states" (together with their antiparticle states) that are the lowest-mass and stablest particle entities, and which furnish the most information as to their generation process. These are the states we focus on in the present studies.

The lowest-mass stable particle is the electron *e*, which is produced from the Higgs field in matching $(e^-, e^+) = 1.022$ MeV pairs. The next observed state is the $(\pi^{\pm}, \pi^0)$ pion doublet, which has an average energy of 137.27 MeV. The energy region between the electron pair and the pion is a void in which no particle states exist. The factor-of-137 ratio between these two energies indicates that the pion mass is created by an "α-leap" up from the electron pair mass. But the electron is a spin $J = 1/2$ lepton and the pion is a spin $J = 0$ hadron. The pion has a quark substructure, and the electron does not. Their masses should be unrelated. The one property they have in common is their *energy*, so the α-leap from the electron to the pion is an *energy* α-*leap*.

The electron is produced in the two-step Higgs generation process shown in Eqs. (8) and (9), in which the *Thomson radius* Higgs energy sphere ${}^{\alpha}S^{ec}_{r_{\rm Th}}$ is transformed into the *Compton radius* Higgs inertial mass sphere ${}^{\alpha}S^{im_e}_{r_c}$. In order to increase the energy of this two-step process by a factor of 137, we extend the radius scaling of Eq. (3) to include the radius $r_{\rm boson}$, so that

$$r_{\rm boson} \times 137 = r_{\rm Thomson}, \quad r_{\rm Thomson} \times 137 = r_{\rm Compton}, \quad r_{\rm Compton} \times 137 = r_{\rm Bohr}\ . \tag{10}$$

The two-step Higgs generation of the boson mass quantum m_b is defined by the equation

$$E^{im_b} = e^2/(r_{\rm Thomson}/137) = e^2/r_{\rm boson} = m_b c^2 \cong 70\ {\rm MeV}, \tag{11}$$

which is the boson counterpart of Eq. (8), and which is half the energy of a pion. The two-step boson alpha-sphere equation is

$${}^{\alpha}S^{ee}_{r_{\rm boson}} \Rightarrow {}^{\alpha}S^{im_b}_{r_{\rm Thomson}}, \tag{12}$$

which in the boson counterpart of Eq. (9), and which represents the adiabatic α-transformation of a 0.2 fm Higgs electrostatic-energy sphere ${}^{\alpha}S^{ee}_{r_b}$ into a 2.8 fm Higgs inertial-mass sphere ${}^{\alpha}S^{im_b}_{r_{\rm Th}}$.

The pion has balanced particle-antiparticle symmetry: it is its own antiparticle. It contains both a particle and an antiparticle substate. We denote the pion symbolically as $\pi = m_b\bar{m}_b$, where the mass quanta $m_b + \bar{m}_b$ are bound together hadronically. Pion production takes place in matching Higgs boson α-leap energy channels from the electron ground state, so that we have

$$boson\ (J=0):\ m_e/\alpha = m_b = 70.025\ \text{MeV}, \tag{13a}$$

$$boson\ (J=0):\ \bar{m}_e/\alpha = \bar{m}_b = 70.025\ \text{MeV}, \tag{13b}$$

Empirically, the Higgs particle energies are calculated most accurately if the boson α-leap energy is added to the (e^-, e^+) ground-state energy, so that the calculated pion mass is 141.07 MeV, which is 2.8% higher than the experimental 137.27 MeV average mass of the $(\pi^{\pm}, \pi^0)$ pion pair. This mass difference is attributed to the hadronic binding energy (HBE) between the m_b and $\bar{m}_b$ pion substates.

The boson energy channel contains the π, η, η' and K pseudoscalar mesons. The K mesons are not particle-antiparticle symmetric, and they carry the *strangeness* quantum number $S = \pm 1$. The π, η and η' mesons are particle-antiparticle symmetric, and they are non-strange (S= 0). An important feature of the π, η and η' pseudoscalar mesons is their very accurate 1::4::7 mass ratio. This means that the boson excitation $m_b\bar{m}_b$ acts as a *unit mass*, wherein the matching α-leaps in Eqs. (13*a*) and (13*b*) are repeated so as to create the higher-energy η and η' mesons. This mass ratio carries over to their particle and antiparticle substates, which are represented as the Higgs energy spheres ${}^{\alpha}S^{im_b}_{r_{\text{Th}}}$, ${}^{\alpha}S^{4im_b}_{r_{\text{Th}}/4}$, and ${}^{\alpha}S^{7im_b}_{r_{\text{Th}}/7}$. These three energy spheres form the pseudoscalar meson inertial-mass quark states $m_{q_\pi} = m_\pi/2$, $m_{q_\eta} = m_\eta/2$ and $m_{q_{\eta'}} = m_{\eta'}/2$, respectively. The energy intervals between these quark masses are each equal to the excitation quantum $X_b \equiv 3m_b \cong 210$ MeV (before the HBE correction is applied). The calculated and experimental mass values for the π, η, η' and K mesons are displayed in Table 7.1.

The spin J = 0 *non-strange* π, η and η' mesons in Table 7.1 contain 2, 8 and 14 m_b and $\bar{m}_b$ total unit masses, respectively. The spin J = 0 *strange* K mesons each contain a total of 7 m_b and $\bar{m}_b$ unit masses, which is an *odd* number. From this it follows that the spin of the m_b unit mass is J = 0, so that m_b is a *boson* constituent quark, as its name suggests.

Table 7.1. The π, η, η' and K pseudoscalar meson energies in units of $m_e = 0.511$ MeV, $m_b = 70.025$ MeV and $X_b \equiv 3m_b = 210.075$ MeV

Energy state	$\pi^{\dagger}$	η	η'	$K^{\dagger\dagger}$
Energy excitation	$2(m_{e+b})$	$2(m_{e+b}+X_b)$	$2(m_{e+b}+2X_b)$	$(m_{e+b}+2X_b)$
Calc. energy (MeV)	141.07	561.2	981.4	490.7
Exp. energy (MeV)	137.27	547.9	957.8	495.6
Calc. accuracy	2.8% †††	2.4%†††	2.5%†††	–1.0%

†ave. $\pi^{\pm}$, π^0 energy; ††ave. $K^{\pm}$, K^0 energy; †††HBE corr. needed.

The accuracy of this $\pi = m_b \bar{m}_b$ unit mass addition process, with its 1::4::7 mass ratio, is illustrated graphically in Fig. 1, where the π, η and η' masses are plotted on a 137 MeV energy grid (which implicitly incorporates the ~2% HBE). The average accuracy of the experimental mass fits to this 137 MeV grid is 0.12%, which attests not only to the energy linearity of these three states, but also to their absolute values.

Fig. 1. The α-quantized nonstrange pseudoscalar meson masses

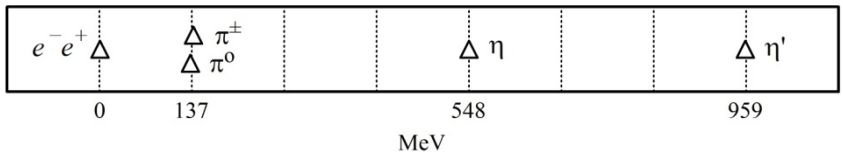

The α quantization of the π, η and η' *masses* is also manifested in their *mean lifetimes*, which are displayed in Fig. 2. This is a plot of lifetimes τ_i relative to the reference $\tau_{\pi^{\pm}}$ lifetime, using a logarithmic lifetime grid spaced by factors of 137. The linear (in powers of 137) π^o, η, η' *lifetime* ratios in Fig. 2 echo the linear π^o, η, η' *mass* ratios in Fig. 1. The significance of these factor-of-137 spacings is that the decaying Higgs energy spheres reflect their quantized two-step α-leap unit-energy build-up.

Fig. 2. The α-quantized nonstrange pseudoscalar meson lifetimes

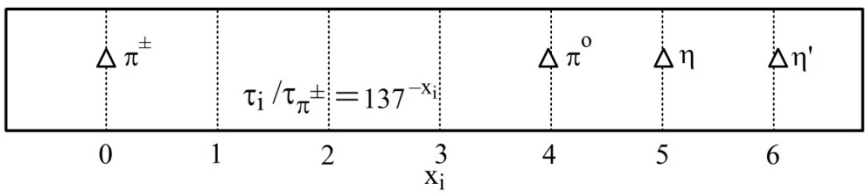

8. The fermion two-step energy channel and the fermion unit mass m_f

The *boson* two-step energy channel features the spin $J = 0$ unit energy quantum $m_b \cong 70$ MeV. If m_b is conceptually set into motion as a Compton-sized relativistically-spinning sphere (RSS), its energy is increased by a factor of 3/2, and its calculated spin is $J = ½\hbar$. It thus becomes the half-integer-spin fermion energy quantum $m_f \cong 105$ MeV. This suggests that m_f serves as the unit energy unit for a *fermion* two-step energy channel which is the counterpart of the boson energy channel discussed in Sec. 7. Confirmation of this suggestion is provided the existence of the 105 Mev μ meson, the muon, which is the lowest-energy fermion above the electron, and which, as we will demonstrate, reflects the unit mass m_f that generates the basic quark and particle fermion ground states. Unlike the boson mass unit m_b, which appears in hadronically bound $m_b\overline{m}_b$ particle-antiparticle energy units, the fermion mass unit m_f appears in separate two-step particle and antiparticle energy channels that are not hadronically bound, and which can be studied separately, so that the energy quantization is more apparent.

The two-step Higgs generation of the mass quantum m_f is defined by the equation

$$E^{im_f} = e^2/(⅔ \times r_{\text{Thomson}})/137 = e^2/r_{\text{fermion}} = m_f c^2 \cong 105 \text{ MeV}, \tag{14}$$

where $r_{\text{fermion}} = (2/3)r_{\text{boson}}$, and is represented by the energy alpha-sphere ${}^{\alpha}S^{im_f}_{r_{⅔\text{Th}}}$. The excitation m_f occurs as an α-leap from the electron ground state, so that we have

$$\textit{fermion}\ (J = 1/2):\ 3m_e/2\alpha = m_f = 105.0375 \text{ MeV}. \tag{15}$$

The unit energy quantum m_f has spin angular momentum $J = 1/2$ as a conserved quantity, and the higher-energy states that it generates are *odd* multiples of m_f, so that the excitation units which add to the m_f ground state must be *even* multiples of m_f. The basic *fermion* excitation unit is $X_f \equiv 2m_f = 210$ MeV, which matches the energy of the *boson* energy excitation unit $X_b \equiv 3m_b = 210$ MeV that appears in the $\pi, \eta, \eta', \text{K}$ boson channel of Table 7.1.

An important difference between the boson and fermion energy excitation channels considered here is that the energy levels in the boson channel are for just one type of particle, the pseudoscalar mesons, but the energy levels in the fermion channel are an interleaved mixture of leptons, quarks, and hadrons, and include two connected excitation sequences: a fundamental

X_f *excitation-doubling* sequence, which is displayed in Table 8.1; and a secondary quark and vector meson *mass-tripling* sequence, which is displayed in Table 8.2.

Table 8.1. Fermion quark and particle excitation-doubling energies in units of $m_e = 0.511$ MeV, $m_f = 105.0375$ MeV and $X_f = 2m_f = 210.075$ MeV

Energy state	μ	*u,d*	*s*	p,n	τ
Energy excitation	m_{e+f}	$m_{e+f}+X_f$	$m_{e+f}+2X_f$	$m_{e+f}=4X_f$	$m_{e+f}=8X_f$
Calc. energy (MeV)	105.55	315.6	525.7	945.9	1786.1
Exp. energy (MeV)	105.66	313.0†	509.7††	938.9†††	1776.8
Calc. accuracy	0.10%	0.8%	3.1%††††	0.7%	0.5%

†ave. p,n energy ÷ 3; ††ϕ meson energy ÷ 2; †††ave. p,n energy; ††††HBE corr. needed.

The excitation sequence in Table 8.1 shows an initial α-leap in energy of $m_e + m_f \equiv m_{e+f}$, followed by an excitation-doubling sequence $n(X_f \equiv 2m_f), n = 0,1,2,4,8$ that creates five Higgs fermion energy levels, which are successively filled as follows: the μ lepton; the (*u.d*) up and down proton-neutron quarks, which are assigned equal masses; the strange quark *s*; the proton-neutron (p,n) average mass; the τ lepton. The three *particle* levels in this excitation ladder—the μ muon, (p,n) nucleon, and τ tauon—have a very accurate 1::9::17 energy ratio, which echoes the accurate 1::4::7 energy ratio of the π, η, η' mesons in Table 7.1. It should be pointed out that the proton and tau lepton mass values, which are accurately reproduced in Table 7.1, are characterized in current Standard Model articles and books as having "no explanation".

The *s*(528) *strange* quark of Table 8.1 acts as a *secondary unit mass*: it generates the

Table 8.2. Fermion (*s,b,c*)quark mass-tripled energies in units of m_e and m_f. Also, vector meson ground states that have decreasing hadronic binding energies (HBE) which vanish above 6 GeV.

Quark state

$$s = m_e + 5m_f = 525.7 \text{ MeV}$$

$$sss = c = m_e + 15m_f = 1576.1 \text{ MeV}$$

$$ccc = b = m_e + 45m_f = 4727.2 \text{ MeV}$$

Vector meson state	$s\bar{s} = \phi$	$c\bar{c} = \mathrm{J/\psi_{1S}}$	$b\bar{c} = \mathrm{B_c}$	$b\bar{b} = \Upsilon_{1S}$
Calc. energy (MeV)	1051.4	3152.2	6303.3	9454.4
Exper. energy (MeV)	1019.5	3096.9	6274.5	9460.3
Calc. accuracy	3.1%†	1.8%†	0.46%	–0.06%

†HBE correction needed.

c(1576) and *b*(4727) *charm* and *bottom* quark inertial masses by successive $s \to c \to b$ mass triplings, as displayed in Table 8.2. These quarks pair together to form the vector meson ground states $s\overline{s} = \phi, c\overline{c} = \mathrm{J/\psi_{1s}}$ and $b\overline{b} = \Upsilon_{1s}$ and mixed-quark excitation $b\overline{c} = \mathrm{B_c}$ shown in Table 8.2. The discrepancies shown between their calculated and experimental mass values reflect the HBE hadronic binding energy that should be applied to the quark-antiquark pair, which is 3.1% for the ϕ at 1 GeV, and then decreases monotonically for the $\mathrm{J/\psi_{1s}}$ and $\mathrm{B_c}$ at increasing energies and vanishes at 9 GeV $b\overline{b} = \Upsilon_{1s}$ and above, as expected from *asymptotic freedom*.

9. The gauge boson two-step energy channel and the gauge boson unit mass m_{gb}

The systematics of the Higgs energy levels in the *boson* energy channel of Sec. 7 establishes the facts that an *α-leap in energy* occurs from the electron mass m_e to the boson mass m_b, and that the mass m_b then functions as a *unit energy quantum* for creating the higher-energy states in that channel. These result are extended by the systematics of the energy levels in the *fermion* energy channel of Sec. 8, where it is shown that the higher-energy levels in that channel, which are created as multiples of the fermion mass m_f, are successively occupied by *different types* of particle states—leptons, quarks, and hadrons—interleaved together. These results are reinforced when we move on the highest-energy particle states—the W and Z gauge bosons and top quark *t*, as we now demonstrate.

The hadron particle states below 12 GeV are reproduced by the *u*,*d*,*s*,*c*,*b* quark states of the Standard Model, so the Higgs masses shown in this energy regime, including the inertial-mass (constituent-quark) values for the quarks, fit into a common Higgs two-step mass generation formalism. However, the high-energy W and Z gauge boson and top quark *t* states, which are above 80 GeV, have no obvious connection to the low-energy regime. The well-investigated energy region from 12 to 80 GeV is devoid of observed particles, which creates a separation between these energy regimes, but which also provides a valuable clue: if these energy regimes have the same Higgs formalism, it involves an α-leap that crosses the 68 GeV particle void.

The key to the Higgs energy structure of these high-mass states is the experimental discovery of a mass relationship between the $(\mathrm{W^{\pm}}, \mathrm{Z^0})$ gauge boson pair and the top quark *t*: [7]

$$m_{\mathrm{W^{\pm}}} + m_{\mathrm{Z^o}} \equiv 2\, m_{\overline{\mathrm{WZ}}} = m_t \ (0.87\% \text{ accuracy}), \tag{16}$$

where $m_{\overline{\mathrm{WZ}}}$ denotes the average energy of the $(\mathrm{W}^{\pm}, \mathrm{Z}^0)$ pair. The accuracy of this mass/energy equation suggests that it is not accidental. It ties together the *energies* of these two types of particle states, which is the one property they have in common. Due to their theoretical importance, a great deal of time and effort has gone into obtaining precise W, Z and *t* mass values. The currently-posted values for these states are [1]

$$\mathrm{W}^{\pm} = 80.385 \text{ GeV};\ \ Z^{\mathrm{o}} = 91.1876 \text{ GeV};\ \ t = 173.07 \text{ GeV}, \tag{17}$$

which gives the average gauge boson energy

$$m_{\overline{\mathrm{WZ}}} = (m_W + m_Z)/2 = 85.79 \text{ GeV}. \tag{18}$$

The *ground state* for the α-leap up to the high-energy regime can be ascertained by analyzing the experiments in which these particles are created. The $\mathrm{W}^{\pm}, Z^0$ and t are produced by p–$\overline{\mathrm{p}}$ collisions at the Tevatron and LHC. At these TeV energies, a proton is flattened relativistically, and the *uud* proton quarks are essentially independent, so the collisions are between individual q_{p} and $\overline{q}_{\overline{\mathrm{p}}}$ quarks, where $q_{\mathrm{p}} = (u, d)$ collectively represents the *u* and *d* proton inertial-mass quarks. (The small *u*-*d* mass difference averages out in the collisions, so that $m_{q_{\mathrm{p}}} = m_{\mathrm{p}}/3$ is an exact relationship.) Once in every 10^{10} scattering events, a head-on $q_{\mathrm{p}}\overline{q}_{\overline{\mathrm{p}}}$ collision occurs where the quark pair absorbs enough collision energy to create gauge bosons and top quarks. If we reproduce this event as an energy α-leap, the factor-of-137 increase in $q_{\mathrm{p}}\overline{q}_{\overline{\mathrm{p}}}$ energy should coincide with the appearance of a particle energy at the calculated α-leap energy, which is

$$(m_q + \overline{m}_{\overline{q}})/\alpha = (m_{\mathrm{p}} + \overline{m}_{\overline{\mathrm{p}}})/3\alpha = 85.72 \text{ GeV}. \tag{19}$$

No direct particle state appears at this energy, but it closely matches the average gauge boson energy of 85.79 GeV shown in Eq. (18). This is agreement to within 0.08%. Hence we have experimentally verified the α-leap energy equation

$$(m_{\mathrm{p}} + \overline{m}_{\overline{\mathrm{p}}})/3\alpha = m_{\overline{\mathrm{WZ}}} \text{ (0.08\% accuracy)}. \tag{20}$$

Using Eq. (16), we can extend this result upwards in energy so as to include the top quark mass, which has the calculated α-leap mass

$$m_t = m_{\mathrm{W}^{\pm}} + m_{Z^0} = 2\,m_{\overline{\mathrm{WZ}}} = 4m_{\mathrm{p}}/3\alpha = 171.44 \text{ GeV}. \tag{21}$$

The measured top quark mass is m_t=173.07 GeV, which matches Eq.(21) to 0.95%. Thus we have experimentally linked the gauge boson average inertial mass and the top quark inertial mass

to the proton quark average inertial mass via the energy α-leap shown in Eq. (19). These equations suggest that it is actually the *average* $\overline{\mathrm{WZ}}$ *energy* that is related to the top quark *t* energy, so that the mechanism which splits the W and Z energies is a separate adiabatic process.

The W gauge boson, like the π boson, has balanced particle-antiparticle symmetry. It is denoted as $\mathrm{W} = m_{gb}\overline{m}_{gb}$, where m_{gb} is the gauge boson unit mass quantum. W production occurs in matching Higgs α-leap energy channels from proton quark ground states, so that we have

$$gauge\ boson\ (J = 1/2):\ m_{u,d}/\alpha = 3m_f/\alpha = m_{gb} = 43.18\ \mathrm{GeV}, \tag{22a}$$

$$gauge\ boson\ (J = 1/2):\ \overline{m}_{u,d}/\alpha = 3\overline{m}_f/\alpha = \overline{m}_{gb} = 43.18\ \mathrm{GeV}. \tag{22b}$$

The m_{gb} quark substate, like the $m_b = 70$ MeV quark substate, is not observed singly. In addition to the calculated energy value for the m_{gb} mass shown in Eqs. (22), we also have the value

$$m_{gb} = m_{\mathrm{p}}/3\alpha = 42.86\ \mathrm{GeV}, \tag{23}$$

which is obtained from Eq. (19), and the experimental value

$$m_{gb} = (m_W + m_Z)/4 = 42.89\ \mathrm{GeV}, \tag{24}$$

which is obtained from Eq. (18). These three slightly different ways of deducing the m_{gb} inertial mass agree to within 0.75%.

In order to preserve spin, charge and other quantum numbers, the top quark *t* must be produced in a matching $t-\overline{t}$ pair, which is a Higgs higher-energy excitation of the $m_{gb}\overline{m}_{gb}$ unit mass pair generated in Eqs. (22a) and (22b). The calculated and experimental mass values for this $t-\overline{t}$ excitation are displayed in Table 9.1. As can be seen, the *gauge boson* excitation sequence in Table 9.1 mirrors the first two energy levels of the *boson* excitation sequence in Table 7.1. At these high energies, the hadronic binding energy HBE is negligible, so the accuracy of the energy calculations is very precise.

Two characteristic features of the Higgs *two-step mass generation process* are (1) an energy α-leap that creates a unit mass *m*, and (2) a multiplication of the mass *m* to create higher-mass levels. Experimentally, this is what occurs in the *gauge boson* energy channel for the $\mathrm{W}^{\pm}, Z^{\mathrm{o}}$ and t high-energy states, so they represent a continuation of the lower-energy Higgs two-step processes for the *boson* and *fermion* energy-channel extraction of energy from the scalar Higgs field in the generation of quark and particle masses.

Table 9.1. The $\overline{\mathrm{WZ}}$ gauge boson and $\mathrm{T} \equiv t\,\bar{t}$ quark pair energies in units of $m_{gb} = 43.18$ GeV and $X_{gb} \equiv 3m_{gb} = 129.54$ GeV

Energy state	$\overline{\mathrm{WZ}}$	T
Energy excitation	$2(m_{gb})$	$2(m_{gb}+X_{gb})$
Calc. energy (GeV)	86.36	345.44
Exp. energy (GeV)	85.79	346.14[†]
Calc. accuracy	0.7%	0.2%

[†]top quark *t* energy × 2

10. Global logarithmic plots of α-quantized ground-state particle masses and lifetimes

The *fermion* mass states contained Tables 8.1, 8.2 and 9.1 are displayed graphically in Fig. 3, using a logarithmic mass scale that is in units of $m_f = 105$ MeV for masses below 12 GeV, and $m_{gb} = 42.86$ GeV for masses above 12 GeV. These masses, together with the *boson* masses of Table 7.1, represent the basic lepton, fermion-quark, and hadron ground states. The unit masses $m_b = 70$ MeV and $m_f = 105$ MeV are produced by α-leaps from the electron, which in turn is produced by an α-leap from the ${}^{\alpha}S^{ee}_{r_{\mathrm{Th}}}$ Higgs energy sphere. The high-energy gauge boson and top quark masses are produced by α-leaps from the proton and antiproton quarks in TeV $\mathrm{p}-\bar{\mathrm{p}}$ collisions. The masses displayed in Figs. 1 and 3 are anchored on the electron mass m_e, and they have calculated absolute mass values that are at an accuracy level of about 1%.

Fig. 3. Fermion plot of quark and ground-state hadron masses.

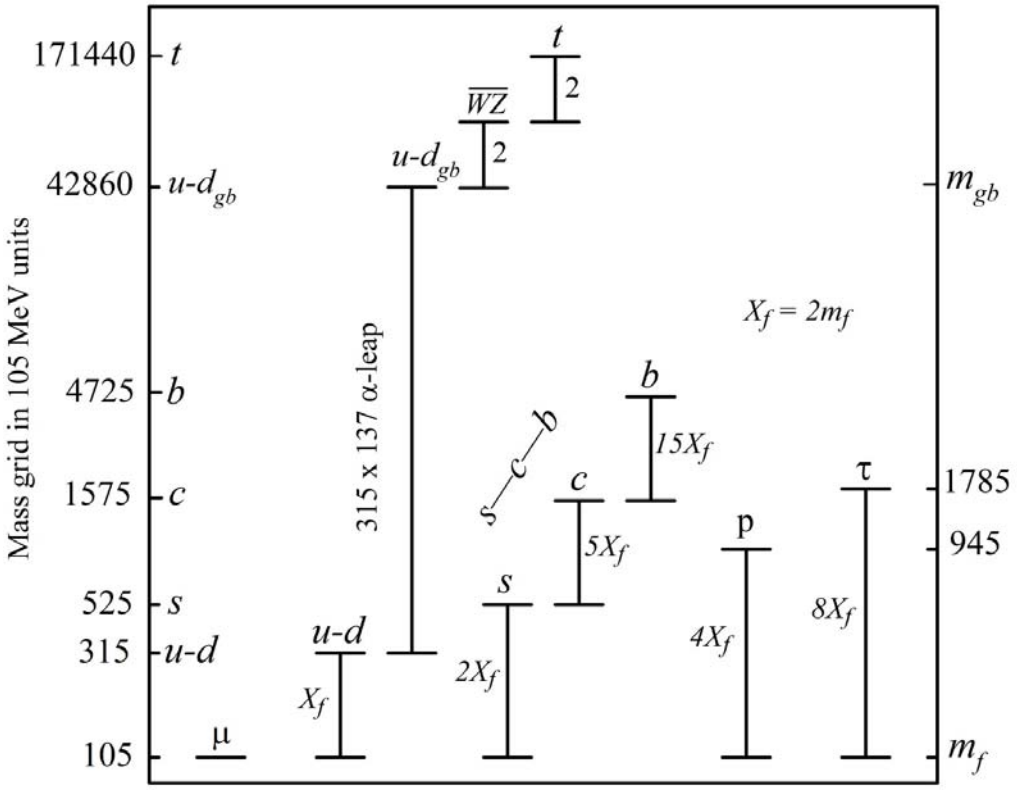

The observed *mass* α-quantization of quark and particle states that is displayed in Fig. 3 is reflected in the *lifetim*e α-quantization of 37 metastable hadrons with lifetimes $\tau > 10^{-21}$ sec that is displayed in Fig. 4. These long-lived particles represent the *ground states* of the leptons and the various hadron quark configurations. Their lifetimes are plotted using the same α-spaced logarithmic lifetime grid and same $\pi^{\pm}$ reference lifetime as in Fig. 2. The lifetimes occur in groups that are each dominated by a single quark flavor—*s*, *b*, *c*. The slow *unpaired-quark* electroweak decays in a group are separated from the fast *paired-quark* decays by a factor of $\sim\alpha^4$, with no intervening lifetimes. These lifetimes demonstrate the extent to which quantizations in factors of $\alpha^{-1} \cong 137$ have permeated the systematics of the metastable ground-state particle lifetimes and masses. [8]

Fig. 4. Lifetime α quantization and α^4 gaps

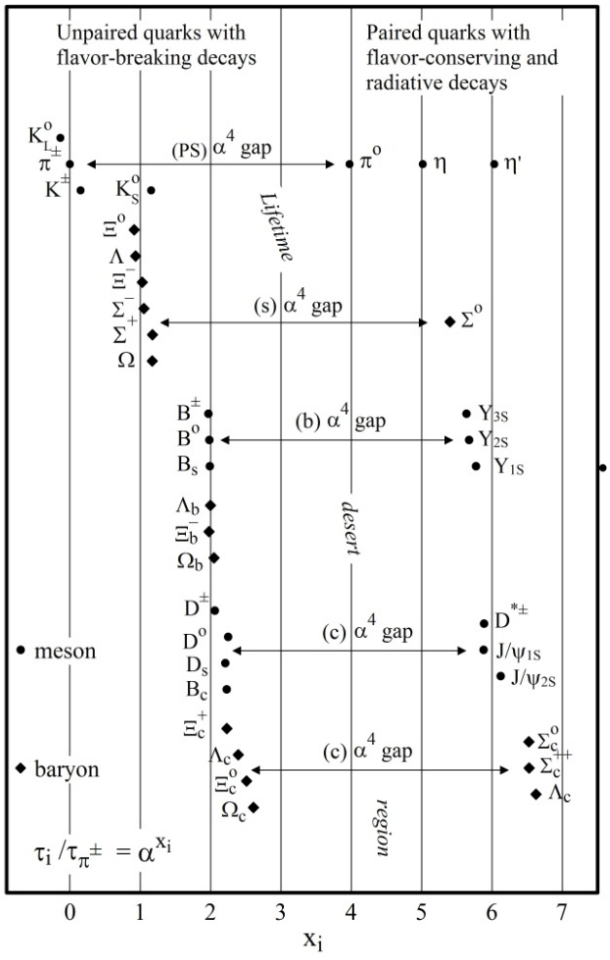

11. Higgs energy streams from the electron to the Υ_{1S} vector meson and the top quark *t*

We conclude with two examples that illustrate the accuracy of the fine structure electrostatic energy and inertial-mass equationss, together with their Higgs energy sphere representations and α-leaps, in calculating electron-based particle energies. Fig. 3 contains an excitation stream of particle energies that starts with the 105 MeV muon and leads up to the *b* quark and the observed $\Upsilon_{1S} = b\overline{b}$ vector meson ground state. Fig. 3 also contains a similar excitation stream that starts with the muon, involves a factor-of-137 Tevatron-LHC α-leap, and leads up to the top quark *t*. The muon itself is reached by a $(3/2\alpha)$ α-leap from the electron. Thus we can start with the electron energy and arrive at both the Υ_{1S} and top quark energies without using any freely-adjustable parameters. The energy stream equation for the Υ_{1S} upsilon mass/energy is

$$m_{\Upsilon_{1S}} = (3/2\alpha)(5)(3)(3)(2)\,m_e = \frac{135}{\alpha}\,m_e = 9453.4 \text{ MeV}. \tag{25}$$

The experimental upsilon mass is [1]

$$\left(m_{\Upsilon_{1S}}\right)_{\text{exper.}} = 9460.3 \text{ MeV}. \tag{26}$$

This is agreement to an accuracy level of 0.07%. The diagram for the energy stream of Eq. (25) is displayed in Fig. 5.

Fig. 5. The energy stream from the electron to the γ_{1S}

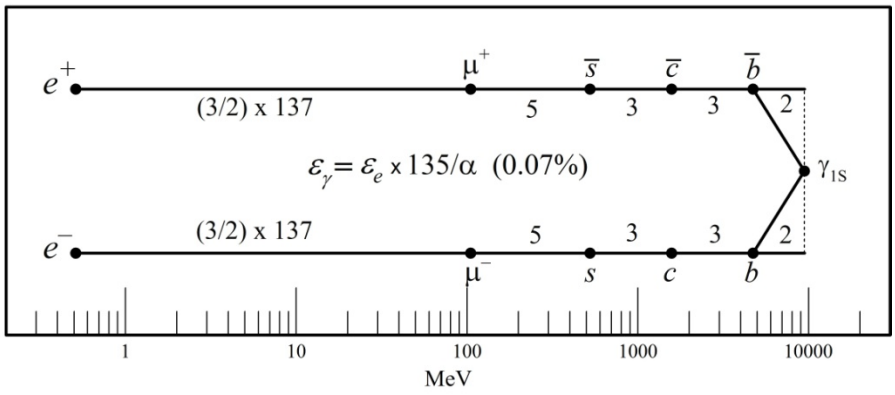

The energy stream equation for the top quark mass is

$$m_{\text{top}} = (3/2\alpha)(9)(1/3)(1/\alpha)(4)m_e = \frac{18}{\alpha^2} m_e = 172.73 \text{ GeV}. \tag{27}$$

The experimental top quark mass is [1]

$$\left(m_{\text{top}}\right)_{\text{exper.}} = 173.07 \text{ GeV}. \tag{28}$$

This is agreement to an accuracy level of 0.20%. The diagram for the energy stream of Eq. (27) is displayed in Fig. 6.

Fig. 6. The energy stream from the electron to the top quark t.

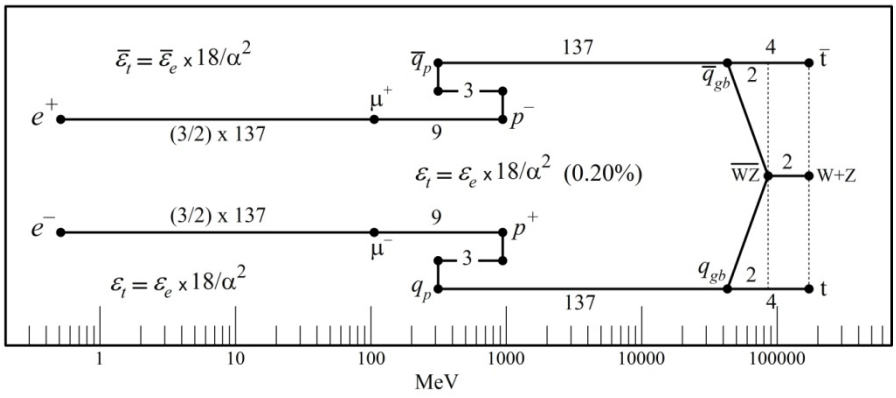

There are two significant conclusions that can be drawn from Eqs. (25-28): (1) The constant α used here is the *renormalized* value $\alpha \cong 1/137,$ and not the running QCD coupling constant $\alpha_s(q^2)$ [9] that increases in value to $\alpha_s(q^2) \approx 1/128$ at $q^2 \simeq m_{\text{W}}^2$. (2) These very accurate parameter-free equations would not be possible without the inclusion of the factor α in Eq. (25) and the factor α^2 in Eq. (27).

If we look beyond the field of elementary particles, then the fact that stored electromagnetic energy expands by a radial factor of 137 when it is converted into particle inertial mass (Eqs. 9 and 12) may be important. On an astronomical scale, the creation of matter may bring with it an expansive thrust that has the attributes of dark energy. The task is to ascertain if the production of the Higgs particle masses, which represent the visible matter that is 4% of the mass in the universe, has contributed significantly to the radially outward motion of the dark energy, which is 76% of the mass in the universe.

References

[1] The mass values and physical constants used in this paper, including the top quark mass, are from J. Beringer *et al*. (Particle Data Group), Phys.Rev. D86, 010001 (2012), and 2013 partial update for the 2014 edition. The cutoff date for this update was January 15, 2013.

[2] M. H. Mac Gregor, *The Enigmatic Electron, 2nd edition* (El Mac Books, Santa Cruz, 2013) and references contained therein to the RSS.

[3] M. H. Mac Gregor, *The Power of Alpha* (World Scientific, Singapore, 2007), Ch. 4.

[4] Ref. [1], pp. 1201-2.

[5] A. Seiden, *Particle Physics* (Addison-Wesley, San Francisco, 2007), pp. 193-200.

[6] M. H. Mac Gregor, arXiv: hep-ph/0603201.

[7] Ref. [3], Appendix A (particle lifetimes) and Appendix B (particle masses), pp. 385-397.

[8] The systematics of particle lifetimes is discussed in detail in Ref. [3], Ch. 2, and in a review article, Int. J. Mod. Phys. A 20, 719-798 (2005), by the present author.

[9] Ref. [1], p. 101; Ref. [5], pp. 234-240.